Dynamic Characterization of Powdered Ceramics*

G. Fenton[1]

[1] Applied Research Associates, 4300 San Mateo Blvd., A-220, Albuquerque, NM 87110

Abstract

The dynamic behavior of powdered materials such as granular silica (sand), technical ceramics, and porous geological substances has importance to a variety of engineering applications. Structural seismic coupling, planetary science, earth penetration mechanics, and the performance of ceramic armors are just some of application areas. Although the mechanical behaviors of sand and other granular ceramics have been studied extensively for several decades, the dynamic behavior over a range of strain rates and pressures of such materials remains poorly understood. This paper describes how instrumented electromagnetic tube compression driven by capacitive discharge can be used to measure compaction of porous materials at moderate pressures and controlled strain rates. The technique relies on electromagnetically crushing a powder-filled conductive tube. By measuring the current as a function of time and the tube displacement through Photon Doppler Velocimetry (PDV) sufficient data can be obtained to reveal the behavior of the porous material. The method will be described in detail and example data will be shown for compaction of silica sand.

Keywords

Dynamic, Compression, Ceramic

1 Introduction

Compression of powdered ceramics falls into a field of science, which has been studied extensively, using both quasi-static and dynamic methods to characterize these materials.

---

* *The author gratefully acknowledges Glenn Daehn and his team at OSU for lab use and experimental work, as well as Tracy Vogler of Sandia National Laboratories for his technical inputs and guidance. Without the financial support granted under Contract PO 208726 from Sandia National Laboratories this effort would not have been possible.*

In this discussion dynamic characterization is obtained through the use of a high-rate technique that does not use an impacting shock wave as the primary consolidation mechanism. This work has similarities to the work of Johnson et al. [1], where expanding materials were investigated.

Investigators have recognized for many years that most materials do not behave the same under static conditions as they do in a dynamic environment. The difference between static and dynamic behavior of powder materials is nicely detailed by Vogler et al. [2]. Scientists have used many different approaches to evaluate the mechanical properties of powder materials under rapid loading. High-quality experimental data is needed for the development of computational models of dynamic material events along with the need to improve our general understanding of dynamic powder material physics.

Dynamic compactions of powder materials typically use shock wave techniques such as explosives or high velocity impactors. This paper describes how instrumented electromagnetic tube compression driven by capacitive discharge can be used to measure pressure-volume relationships for model materials at high and controlled strain rates. By measuring the driving current as a function of time and the tube displacement through Photon Doppler Velocimetry (PDV) based on Strand et al. [3,4], the behavior of the porous material can be revealed. The electromagnetic compression technique affords the investigator symmetric loading, repeatability, and precise energy input which is why this technique is being used to obtain high rate low-pressure data [5]. This data is used to validate the P-λ equation-of-state [6] for describing the compaction of porous granular media at the continuum level.

2 Experimental Concepts

2.1 Traditional Methods

The traditional methods used to dynamically compress porous materials usually involve explosives and/or high velocity drivers where direct and intense shock waves achieve compression. These methods while effective at compression can have undesirable attributes associated with them. For example, the methods can be time consuming to perform and usually require expensive testing to obtain accurate and reproducible data. In addition, it is difficult to control the delivery of the compacting energy and maintain the reproducibility of the energy delivery to the material sample over a sequence of experiments.

2.2 An Alternative Method

The Photon Doppler Velocimetry is an enabling technology for porous material compression testing, as velocity is a key parameter in modeling. A heterodyne velocimetry system based on the work of Strand et al. [2,3] was constructed for channels of velocity data at peak velocities under 1000 m/s. The system was used successfully to measure velocities of electromagnetically compressed axisymmetric samples. The low cost methodology illustrated in Figure 1 has contributed useful data to determine material properties under high strain rates and benchmarks for numerical analysis of porous material compaction.

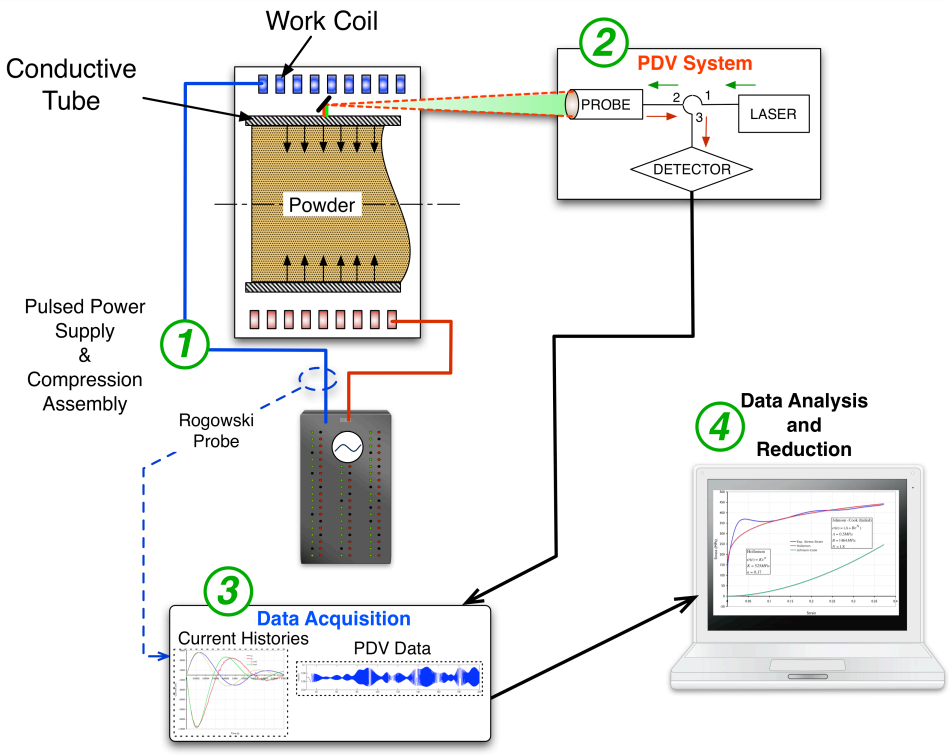

***Figure 1**: Electromagnetic compression system for porous material compaction.*

The compression system shown above, consists of four main components: 1) Power supply and work coil; 2) PDV system; 3) Data acquisition; and 4) Data analysis software. A specimen is placed in the work coil and a high frequency electrical discharge is released into the coil to dynamically compress the specimen at high strain rates $(10^2 s^{-1}$ to $10^4 s^{-1})$ within an axisymmetric strain field. The high strain rates are achieved due to the intense interaction of opposing Lorentz forces acting between the conductive tube and the work coil. The interacting Lorentz forces can create magnetic pressures, which may reach upwards of 500 MPa for this test configuration.

3 Mechanics of Alternative Method

This section describes the mechanics of the EM technique, which are needed to perform analysis of the data obtained from the EM compression experiment. The required information consists of material information about the conductive tube, initial bulk density of the sample material, resistance-inductance-capacitance (RLC) values about the capacitor system (this can be resolved from the time-history waveform of the driving current and are assumed to remain constant during the experiment), and lastly the velocity time history of the conductive tube (this is determined from the processed data signal obtained by the PDV system).

To gain understanding of the system operation, the system can be described as a capacitive discharge unit connected to a coil. The coil delivers the magnetic energy to the sample tube. This configuration mimics a series RLC circuit mutually coupled to an RL circuit. Figure 2 illustrates this coupled circuit concept. Kirchhoff loop laws may be applied to the circuits in Figure 2 to obtain ordinary differential equations, which relate the external circuit to the changing sample tube circuit.

Primary current (I_1) induces an Eddy current (I_2) in the tube. The interactions of the currents cause a repulsive force (F_m). The mutual inductance governs the electromagnetic coupling and the magnetic force generated (F_m).

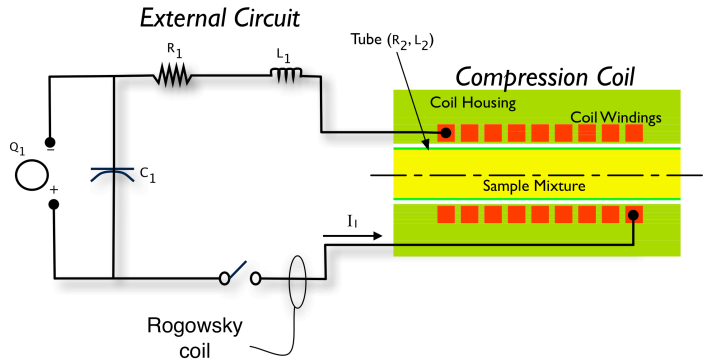

***Figure 2**: Compression system circuit schematic. Consists of two mutually coupled circuits, the external driving circuit plus the compression coil (subscript 1) and the sample tube (which will be subscript 2 in further reading).*

Kirchoff's loop rule was used to sum the voltages across the elements in the coupled circuit shown in Figure 2. The loop law yields the ordinary differential Equations 1 and 2.

$$\frac{d}{dt}\left(L_1 I_1 + M I_2\right) + R_1 I_1 + \frac{Q_1}{C_1} = 0 \tag{1}$$

$$\frac{d}{dt}\left(L_2 I_2 + M I_1\right) + R_2 I_2 = 0 \tag{2}$$

Equation 1 is the sum of the voltages around the primary circuit (external circuit + coil). Equation 2 is the sum of the voltages around the secondary circuit (tube). According to Lenz's Law the induced current in the tube is always in a direction as to oppose the cause that produced it. Hence, a plus sign results in front of the MI_2 and the MI_1 terms found in the two differential Equations 1 and 2. To obtain the total time derivatives of the currents I_1 and I_2 the product rule of differentiation and Cramer's rule were used. This resulted in two total time derivatives of current in the coil,

$$\dot{I}_1 = \frac{\dot{M}\left(L_2 I_2 - M I_1\right) + L_2\left(\frac{Q_1}{C_1} + R_1 I_1\right) - M I_2\left(R_2 + \dot{L}_2\right)}{M^2 - L_2 L_1} \quad , \tag{3}$$

and the tube,

$$\dot{I}_2 = \frac{\dot{M}\left(L_1 I_1 - M I_2\right) + L_1 I_2\left(\dot{L}_2 + R_2\right) - M\left(R_1 I_1 + \frac{Q_1}{C_1}\right)}{M^2 - L_2 L_1} \quad . \tag{4}$$

An energy balance between the two circuits exists, which allows for an expression of the magnetic force (F_m) acting between the coil and the conductive tube,

$$F_m = \frac{1}{2}\frac{dL_2}{dr} I_2^2 + \frac{dM}{dr} I_1 I_2 \quad . \tag{5}$$

The mutual inductance term M and the self-inductance L_2 of the tube are critical items for properly calculating the motion of the tube wall. The self-inductance and the mutual inductance of the tube are assumed to follow the induction relations from Rosa and Grover [7].

Looking only at the sample tube for now, the sample tube can be considered to be a thin walled structure with flow strength and magnetic pressure (P_m) acting on the outside of the tube, as well as resistive compaction pressure (P_c) from the granular material acting on the inside of the tube. This concept allows for the development of a free-body-diagram of forces acting on a differential element of the conductive tube. Figure 3 illustrates the pressures involved in relation to the geometry of the sample tube, which leads to the free body diagram also shown in Figure 3.

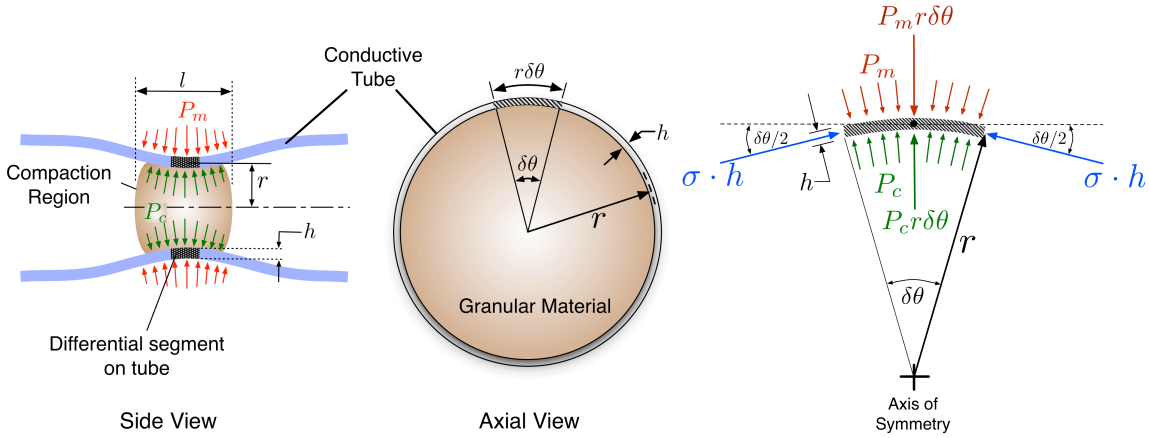

***Figure 3**: Pressure acting on sample tube and the assumed tube geometry with a free body diagram of forces acting on a differential element of the tube.*

Summing the radial forces acting on the differential element of the tube provides an equation of motion for the tube element. Equation 6 is the tube radial equation of motion. P_m and P_c are the magnetic and compact pressures acting on the tube. σ is the material flow stress of the tube, which is assumed to be a known relationship to the radial strain in the tube. ρ is the tube material density. Variables h_o and r_o are the tube initial wall thickness and initial wall radius respectfully. $r(t)$ is the radial location of the tube as a function of time. The radial motion of the tube wall is measured by the PDV system, which is how $\ddot{r}(t)$ and $r(t)$ is determined for inclusion into Equation 6.

$$\ddot{r}(t) = \frac{(P_m - P_c) r(t)^2}{\rho\, h_o r_o^2} - \frac{\sigma}{\rho\, r(t)} \quad . \tag{6}$$

The primary current history (I_1) is measured using a Rogowski probe. Given the radial velocity, and therefore the radial displacement as well as I_1 are all measured as a function of time, the magnetic pressure between the coil and the tube is solvable.

$$P_m = \frac{\frac{1}{2}\frac{dL_2}{dr} I_2^2 + \frac{dM_{12}}{dr} I_1 I_2}{2\pi\, r(t)\, l} \tag{7}$$

Equation 7 gives the magnetic pressure; the radial equation of motion can be turned around and solved for the nominal compact pressure at the interface of the granular material and the conductive tube. Equation 8 gives the nominal compact pressure,

$$P_c = P_m - \frac{h_o r_o^2}{r(t)^2}\left(\rho\, \ddot{r}(t) + \frac{\sigma}{r(t)}\right) \quad . \tag{8}$$

The data obtained from a compression test consists of the primary current recorded by a Rogowski coil and the free surface velocity of the tube measured by Photon Doppler Velocimetry (PDV). Figure 4 illustrates a typical data set obtained from a compression experiment. The top plot in Figure 4 is raw PDV data. The middle plot is a Fourier reduced signal from the raw PDV data, which renders a radial velocity history of the tube outer wall. The bottom plot in Figure 4 is the primary current which is the driver of the compression test. With the primary current measured and applying assumptions about the inductance of the experimental setup the magnetic pressure can be calculated from Equation 7. The velocity of the tube wall is measured over time, which means we can differentiate and integrate the PDV data to provide radial acceleration and radial location of the tube. Using an assumed flow stress model for the tube material, the calculated magnetic pressure, the radial location, the radial acceleration, and the nominal compact pressure within the powder material can be computed through the use of Equation 8.

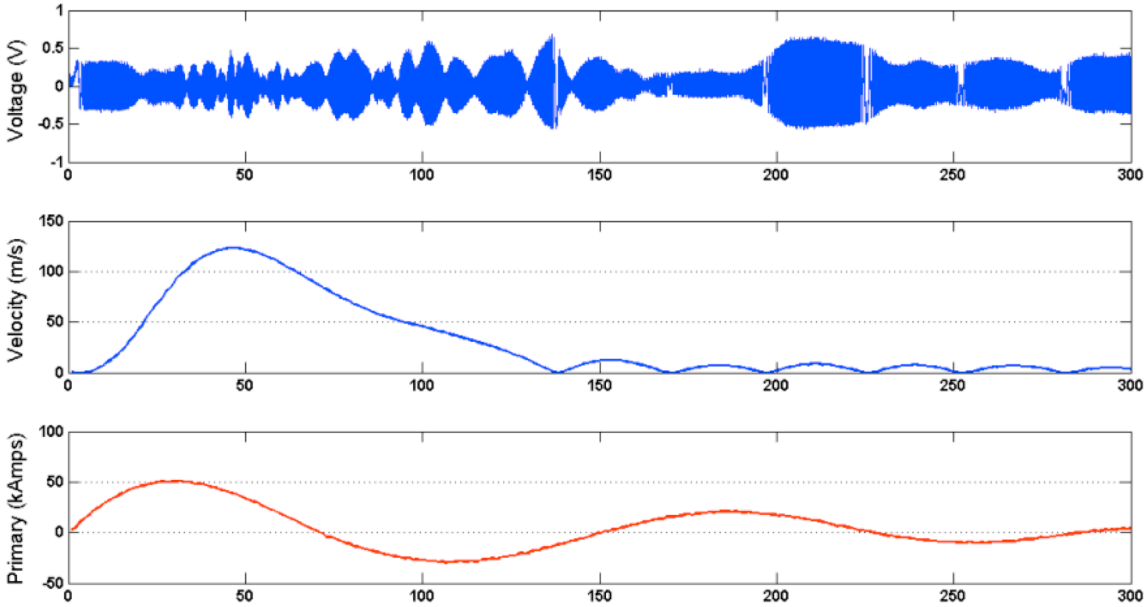

***Figure 4**: Typical data obtained from EM compression experiment.*

4 Equation of State Model

Numerical methods have proven extremely effective in computing the detailed dynamic deformation of materials in a wide variety of different geometries and under many different loading conditions. As such they are ideally suited for the detailed study of stress wave interactions during and after the consolidation of porous materials. We have chosen the CALE code, a two-dimensional (2D) Arbitrary Lagrangian Eulerian (ALE) wave interaction computer program [8] due to its unique capabilities for modeling magneto hydrodynamics and mechanical deformation in a coupled manner.

A number of computational models have been developed to treat the dynamic compaction of porous media. However, predicting the response of a heterogeneous mixture of materials, which most powders constitute, is difficult. The constitutive response of solids is commonly decomposed into the equation-of-state (volumetric) and strength response (deviatoric). Microstructure properties such as grain size, porosity, and multiple phases play an important role in the strength of porous materials. Not commonly recognized is that the same microstructure properties can also influence the volumetric response of powders leading to volumetric hysteresis and dissipation. The purpose of the P-λ equation-of-state is to only encompass the volumetric response. Our approach is focused on the dynamic response of a mixture of materials (including porosity) with wide disparities in density, strength, and compressibility. The model is intended to be robust for both computational and analysis applications. Above all, the model is intended to provide a first-order dynamics response of the material with relatively few material properties. This follows the philosophy of the P-α model, described by Herrmann [9] and, by Carroll-Holt [10].

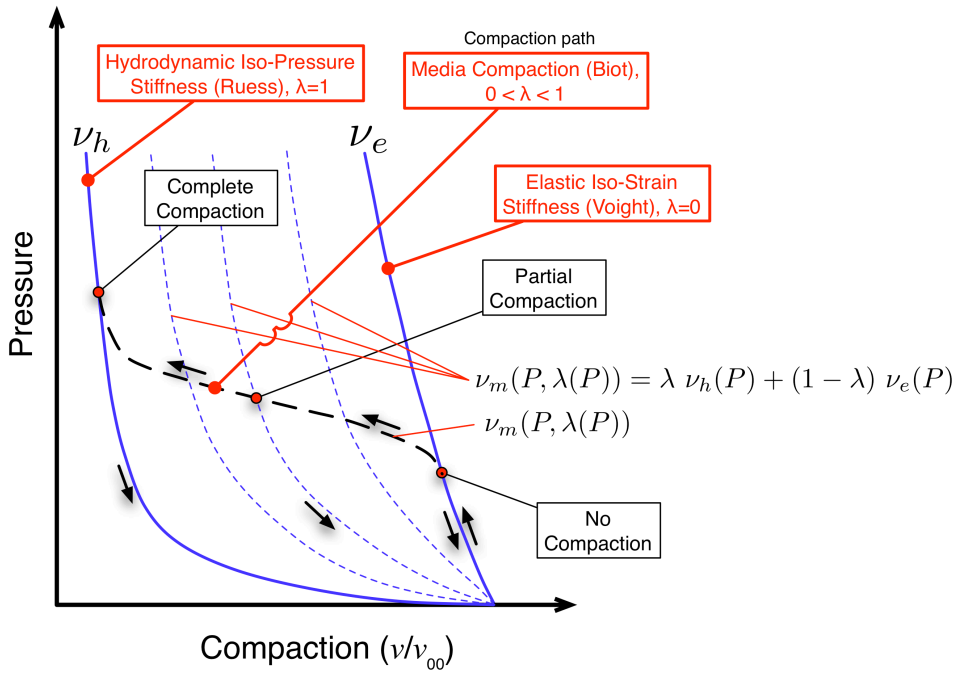

***Figure 5**: The P-λ model illustrated in P-V space.*

Figure 5 illustrates the P-λ computational model, which was developed for describing the compaction of heterogeneous media (in this case a mixture of silica and air). The P-λ material equation-of-state [6] is suitable for distended mixtures of powdered

solids (base material) and interstitial fluid (matrix material) such as water, air, or vacuum. It is intended to model compaction behavior under extreme pressure loadings. It is based on the superposition of specific volume,

$$\text{Compaction of mixture}(P) \equiv \frac{v_m(P)}{v_{oo}} = \lambda(P)\ \frac{v_h(P)}{v_{oo}} + (1-\lambda(P))\ \frac{v_e(P)}{v_{oo}} \tag{9}$$

where $v_h(P)$ and $v_e(P)$ are elastic compression relations for the fully compacted solid media (iso-pressure curve) and the initially distended media (iso-strain curve), respectively. The parameter λ is a pressure dependent function ranging from "0" for the initial un-compacted media to "1" for the fully compacted material. The functional form (Equation 10) currently used for λ is based on a Weibull statistical strength of materials concept, where σ and n are compaction parameters in this representation,

$$\lambda(P) = 1 - e^{-\left(P/\sigma\right)^n} \tag{10}$$

and P is the pressure or stress. The σ parameter is related to the strength of the mixture at a granular level, which roughly controls the point of departure from iso-strain behavior. The n parameter represents the homogeneity of compaction which relates to the abruptness of the transition to iso-pressure behavior. The effects of the parameters are illustrated in the Figure 6.

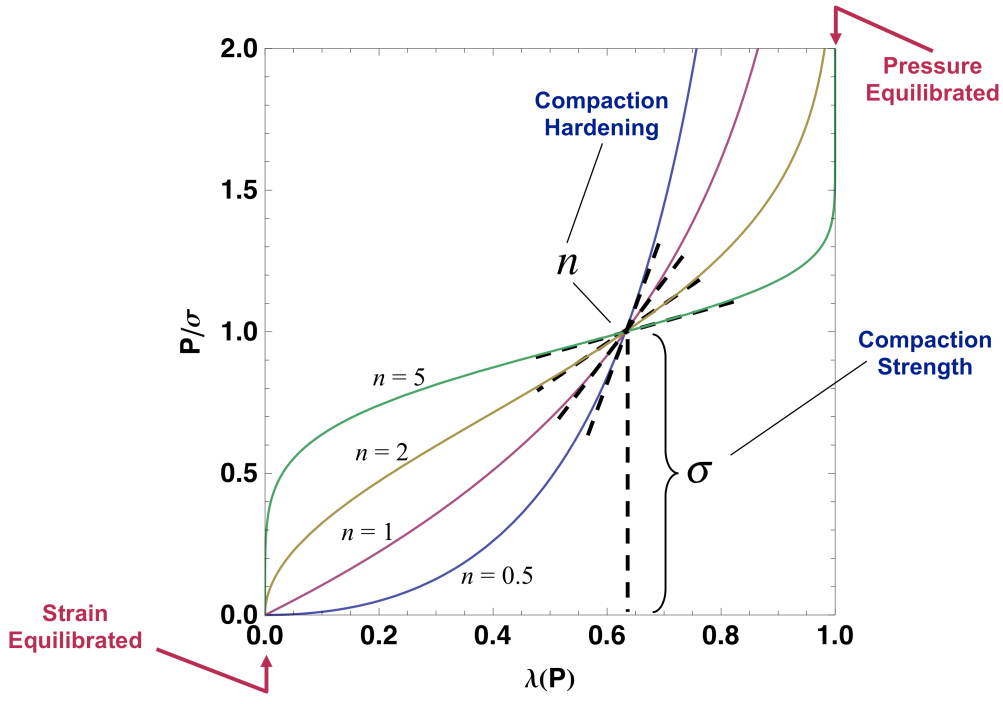

***Figure 6**: Compaction parameters of the exponential P-λ model.*

The specific values of σ and n are obtained through a least squares regression of the compression data and it is assumed you know some characteristics of the components of the powder mixture, specifically the granular volume fractions, densities, sound speeds, and the slopes of the linear $U_s - u_p$ Hugoniot equation of state.

5 Results

A sand compaction simulation was performed in CALE [8]. The P-λ equation-of-state for the sand was taken from the investigative work performed by Brown et al. [11]. In this work they performed a number of high velocity gas gun experiments, which resulted in a locus of Hugoniot data points from which a P-λ model was derived. The P-λ model parameters (as seen in Equation 10) were determined to be a $\sigma = 0.115$ GPa and $n = 0.3$. This model was implemented in CALE and run with a poloidal magnetic field option, which compressed the sample tube. Results of the simulation and experiment are shown in Figure 7.

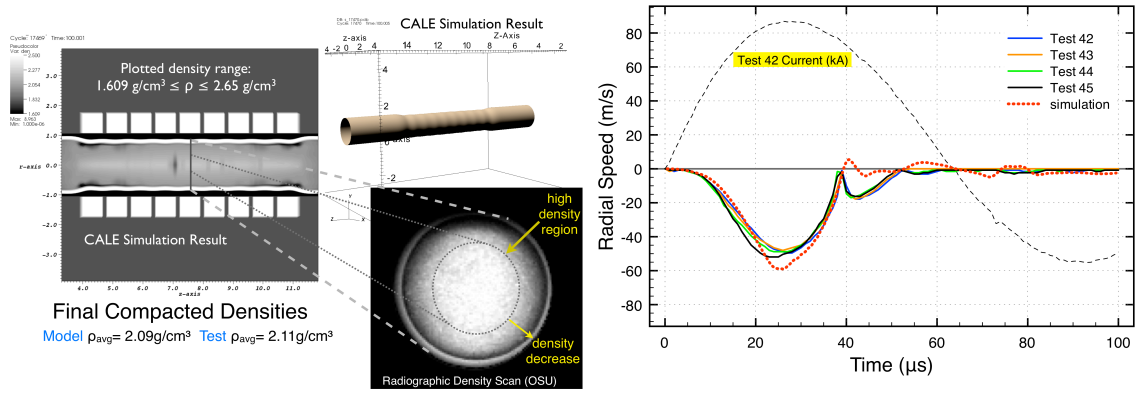

***Figure 7**: Computational and experimental results of a compression test.*

Velocity data taken from the PDV system is plotted in Figure 7 for several tests. These tests were conducted at the same initial bulk packing density and the same driving current. The primary current from Test 42 is shown in units of kilo-amps to illustrate the relative timing of the driving current as compared to the velocity of the compressing tube wall. Figure 7 also shows the apparent reproducibility of data from test to test, as well as the good agreement between the experimental and the simulated tube velocity. Figure 7 illustrates how well the P-λ model aids in describing the dynamic response of the sand filled tube.

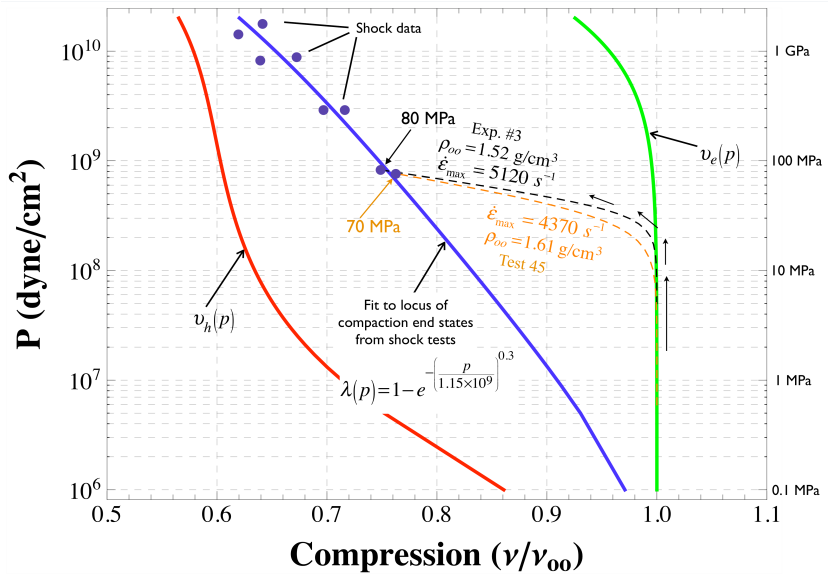

***Figure 8**: Pressure vs. Compression plot for silica sand.*

Figure 8 portrays a lot of information about the compression of dry silica sand. The pressure levels displayed span many decades from very low to moderately high. The black and orange dashed curves are overlaid results of two EM compression tests. These curves represent compaction paths as well as final compaction end states for the sand. The end points of the EM compression curves fall very close to the extrapolated shock data fit. The orange and black curves were two separate and unique experiments on the same material. The fact that the end points from the EM compression tests are nearly the same, suggests that the test technique has invariance to sample configuration.

6 Conclusions

Both experimental and computational studies of the compaction of silica were explored. The PDV technique was used successfully to measure compression velocities of EM compressed samples. This method has contributed useful validation data of mixture compaction under high strain rates and benchmarks for numerical analysis of porous material compaction. The EM technique has proved to be successful in determining low pressure Hugoniot response of mixtures showing simulation and experiment agree well with each other.

References

[1] *Johnson, J.R.; Taber, G.; Vivek, A.; Zhang, Y.; Golowin, S.; Banik, K.; Fenton. G.K.; Daehn, G.S.; Coupling Experiment and Simulation in Electromagnetic Forming Using Photon Doppler Velocimetry, Steel Research Int., 80, 359-365, (2009).*

[2] *Vogler, T.J.; Lee, M.Y.; Grady, D.E.; Static and Dynamic Compaction of Ceramic Powders, Int. J. of Solids and Struct., 44, 636-658 (2007).*

[3] *Strand, O.; Berzins, L.; Goosman, D.; Kuhlow, W.; Sargis, P.; and Whitworth, T.; In 26th International Congress on High-Speed Photography and Photonics, edited by D. Paisley, (SPIE, Alexandria, VA), Vol. 5580, p. 593, (2004).*

[4] *Strand, O.; Goosman, D.; Martinez, C.; and Whitworth, T.; Rev. Sci. Instrum. 77, 83108, (2006).*

[5] *Fenton, G.; Caipen, T.; Daehn, G.; Vogler, T.; Grady, D.; Shock-less High Rate Compaction of Porous Brittle Materials, AIP Conference Proceedings, SHOCK COMPRESSION OF CONDENSED MATTER, Volume 1195, pp. 1337-1340 (2009).*

[6] *Grady, D.E.; Winfree, N.A.; Kerley, G.I.; Wilson, L.T.; Kuhns, L.D.; Computational Modeling and Wave Propagation in Media with Inelastic Deforming Microstructure. Journal de Physique IV 10, 15–20, (2000).*

[7] *Rosa E. B. and Grover F. W., Formulas and Tables for the Calculation of Mutual and Self Induction," [Revised], Bulletin of the Bureau of Standards, Vol. 8, No. 1, 1911, p. 122.*

[8] *R. E. Tipton; A 2D Lagrange MHD Code. In 4th Int. Conf. on Megagauss Magnetic Field Generation and Related Topics, page 299, New York, 1987. Plenum Press.*

[9] *Herrmann, W.J.; Appl. Phys., 40, 2490-2499 (1968).*

[10] *Carroll, M.M. and A.C. Holt; J. Appl. Phys., 43, 1626-1635 (1972).*

[11] *Brown, J.L.; Vogler, T.J.; Grady, D.E.; Reinhart, W.D.; Chhabildas, L.C.; Thornhill, T.F.; Dynamic Compaction of Sand, AIP Conference Proceedings, SHOCK COMPRESSION OF CONDENSED MATTER, Volume 955, pp. 1363-1366 (2007).*